Journal of Materials Chemistry B

ROYAL SOCIETY OF CHEMISTRY

PAPER

View Article Online
View Journal | View Issue

Cite this: J. Mater. Chem. B, 2024, 12, 1538

Biocatalytic nitric oxide generating hydrogels with enhanced anti-inflammatory, cell migration, and angiogenic capabilities for wound healing applications†

Phuong Le Thi,‡[ab] Dieu Linh Tran,‡[bc] Kyung Min Park,[d] Simin Lee,[e] Dong Hwan Oh[e] and Ki Dong Park*[e]

Although wound healing is a normal physiological process in the human body, it is often impaired by bacterial infections, ischemia, hypoxia, and excess inflammation, which can lead to chronic and non-healing wounds. Recently, injectable hydrogels with controlled nitric oxide (NO) release behaviour have become potential wound healing therapeutic agents due to their excellent biochemical, mechanical, and biological properties. Here, we proposed novel multifunctional NO-releasing hydrogels that could regulate various wound healing processes, including hemostasis, inflammation, cell proliferation and angiogenesis. By incorporating the copper nanoparticles (NPs) in the network of dual enzymatically crosslinked gelatin hydrogels (GH/Cu), NO was *in situ* produced *via* the Cu-catalyzed decomposition of endogenous RSNOs available in the blood, thus resolving the intrinsic shortcomings of NO therapies, such as the short storage and release time, as well as the burst and uncontrollable release modes. We demonstrated that the NO-releasing gelatin hydrogels enhanced the proliferation and migration of endothelial cells, while promoting the M2 (anti-inflammatory) polarization of the macrophage. Furthermore, the effects of NO release on angiogenesis were evaluated using an *in vitro* tube formation assay and *in ovo* chicken chorioallantoic membrane (CAM) assay, which revealed that GH/Cu hydrogels could significantly facilitate neovascularization, consistent with the *in vivo* results. Therefore, we suggested that these hydrogel systems would significantly enhance the wound healing process through the synergistic effects of the hydrogels and NO, and hence could be used as advanced wound dressing materials.

Received 24th August 2023,
Accepted 2nd January 2024

DOI: 10.1039/d3tb01943h

rsc.li/materials-b

Introduction

Cutaneous injuries, including chronic wounds, burns and infectious wounds, are increasing severely and becoming urgent, high-cost healthcare problems worldwide. In particular, elderly and diabetic patients suffer from abnormal and long-term wound healing because of the associated complications, such as neuropathy, ischemia, and infection, which may lead to amputation and even mortality.[1,2] To address these challenges, various strategies using wound healing materials and delivery systems have been explored to accelerate the wound healing process, which include nanofibers, nanoparticles, microgels/hydrogels, micelles, composites, foams, and spongy/bilayered/trilayered scaffolds.[3,4] Among these materials, hydrogels offer attractive advantages for wound healing owing to their highly hydrated 3D porous network that can absorb the wound exudates and allow the exchange of oxygen and nutrients to accelerate healing. Interestingly, *in situ* forming hydrogels have been proposed as attractive hydrogel formulations, because of their ability to fill any irregular defect and easy encapsulate therapeutic drugs in the pre-gel solution.[5–9]

The wound healing process generally consists of four continuous overlapping phases that involve dynamic interactions between various types of cells and their products, bioactive

[a] Institute of Applied Materials Science, Vietnam Academy of Science and Technology, No. 1B – TL29 Street, Thanh Loc Ward, 12th District, Ho Chi Minh City 700000, Vietnam. E-mail: ltphuong@iams.vast.vn
[b] Graduate University of Science and Technology, Vietnam Academy of Science and Technology, Ho Chi Minh City 700000, Vietnam
[c] Institute of Chemical Technology, Vietnam Academy of Science and Technology, No. 1A – TL29 Street, Thanh Loc Ward, 12th District, Ho Chi Minh City 700000, Vietnam. E-mail: tdlinh@ict.vast.vn
[d] Department of Bioengineering and Nano-Bioengineering, Incheon National University, 119 Academy-ro, Yeonsu-gu, Incheon 22012, Republic of Korea. E-mail: kmp@inu.ac.kr
[e] Department of Molecular Science and Technology, Ajou University, Suwon 16499, Republic of Korea. E-mail: lsm0428@ajou.ac.kr, slapbass00@ajou.ac.kr, kdp@ajou.ac.kr

† Electronic supplementary information (ESI) available. See DOI: https://doi.org/10.1039/d3tb01943h

‡ These authors contributed equally to this work.

factors, and extracellular matrices (ECMs): hemostasis, inflammation, proliferation, and remodeling. During these phases, hydrogels integrated with bioactive agents (drugs/cells/peptides/proteins/genes) can contribute to promoting the wound healing process.[4,10,11] Among bioactive compounds, nitric oxide (NO) demonstrated tremendous therapeutic potential to regulate various wound healing processes, including inflammatory response, cell proliferation, collagen formation, antimicrobial action, and angiogenesis.[12–15]

However, due to its short half-life and sensitivity to external factors (*e.g.*, temperature, pH, light, and metals), NO demands a storage and delivery system to protect its stability, biocompatibility, retention time and bioavailability. Injectable hydrogels have emerged as ideal delivery candidates for the controlled and sustained release of NO, thereby facilitating a synergistic effect in wound healing. So far, different types of injectable NO-releasing hydrogels have been designed by physically or chemically incorporating NO donors (*e.g.*, diazeniumdiolates, *S*-nitrosothiols, nitrosamines, and nitrites) into the hydrogel matrix.[15–19] Although physical incorporation of NO donors is a simple process without requiring additional reaction or modification steps, the premature and unspecific release of the NO donors from the hydrogel matrix is extremely undesired. In contrast, hydrogels with chemically attached NO donors involve complex reactions but offer the advantage of preventing leaching and precocious NO release due to unwanted NO donor decomposition. Recently, biocatalytic NO generating hydrogels that have the ability to produce NO *in situ* upon contact with blood have attracted substantial attention. These hydrogels are equipped with biocatalysts or biomimetic catalysts to act on endogenous nitrite/nitrate or nitrosothiols within the blood. This mechanism induces a local increase in NO levels at the implanted sites. Unlike the physical incorporation or chemical attachment of synthetic exogenous NO donors, this approach utilizes available NO reservoirs and triggers within biological systems, resulting in local, sustainable, and long-term NO release.[12,14,20]

Herein, for the first time, injectable biocatalytic NO generating hydrogels are created by using the dual-enzymatic crosslinking of horseradish peroxidase (HRP) and tyrosinase (Tyr), which provide multiple functions for wound healing applications. First, the HRP/Tyr-mediated crosslinking forms an injectable formulation and enhances the tissue adhesiveness of the resulting hydrogel, which allows it to firmly adhere to the open wounds, thus covering the open wounds. Secondly, in the presence of copper ions (Cu^{2+}), this approach enables the formation of copper nanoparticles (Cu NPs) within the hydrogel matrix through the redox-reaction between Cu^{2+} and Tyr-induced catechol groups, subsequently producing *in situ* NO *via* the Cu-catalyzed decomposition of endogenous RSNOs in the blood (Fig. 1). We demonstrate the therapeutic potential of NO-producing hydrogels that enhance the proliferation and migration of endothelial cells and promote the M2 (anti-inflammatory) phenotype of macrophages for enhanced wound management. Moreover, we confirmed the hydrogels' angiogenic properties, including *in vitro* tube formation and *in ovo* neovascularization. Finally, we evaluate the bioactivity and angiogenic potency of these injectable NO-releasing hydrogels in animal models. Taken together, our results suggest the great potential of injectable NO-releasing hydrogels with high tissue adhesion, cell proliferation and migration, and enhanced anti-inflammatory and angiogenic capabilities for wound healing applications.

Experimental

Materials

Gelatin (type A from porcine skin, >300 Bloom), 3-(4-hydroxyphenyl) propionic acid (HPA), 1-ethyl-3-(3-dimethylaminopropyl)-carbodiimide (EDC), *N*-hydroxy-succinimide (NHS), peroxidase from horseradish (HRP type VI, 250–330 U mg^{-1} solid), hydrogen peroxide (H_2O_2), copper sulfate ($CuSO_4$, ≥99%), and tyrosinase from mushroom (Tyr, 3610 units mg^{-1} solid)

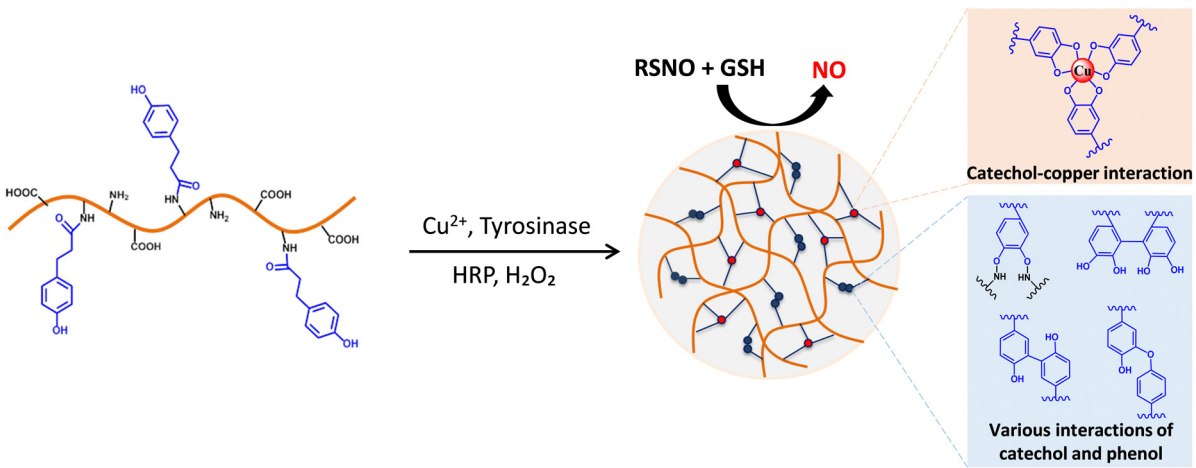

Fig. 1 Schematic diagram representing the formation of a nitric oxide releasing hydrogel through the catalysis of horseradish peroxidase and tyrosinase. The GH polymer was crosslinked *via* various interactions between catechol and phenol groups.

were obtained from Sigma-Aldrich (St. Louis, MO, USA). Dimethylformamide (DMF) was obtained from Junsei (Tokyo, Japan). Penicillin–streptomycin (P/S), trypsin/ethylenediaminetetraacetic acid (TE), and Dulbecco's phosphate-buffered saline (DPBS) were purchased from Gibco BRL (Grand Island, NY, USA). Human Umbilical Vein Endothelial Growth Medium (CEFOgro-HUVEC) was purchased from CEFO (Gyeonggi, Korea). Phorbol 12-myristate 13-acetate (PMA), IFN-gamma Recombinant Human Protein (IFN-γ), interleukin 4 (IL-4) and interleukin 13 (IL-13) (recombinant human) were ordered from PeproTech (Korea). The EZ-Cytox enhanced cell viability assay kit (WST-1 assay reagent) was purchased from ITSBIO (Seoul, South Korea). The CD163 polyclonal antibody was obtained from Invitrogen (California, USA). Other chemicals and solvents were used without further purification.

Preparation and gelation time of the GH/Cu hydrogel

Gelatin-hydroxyphenyl propionic acid (GH) was synthesized through carbodiimide chemistry and characterized as described in our previous study.[21,22] To prepare the GH/Cu hydrogel, the GH polymer was completely dissolved in DIW at 37 °C at a concentration of 6.25 wt%. In a 1.5 mL microtube, GH solution was mixed with HRP (0.025 mg mL^{-1}) and Tyr (2.5 kU mL^{-1}) solutions. In another microtube, GH polymer solution was mixed with H_2O_2 (0.2 wt%) and $CuSO_4$ with concentrations of 0, 250, 500, and 750 μM. The final concentrations of HRP, Tyr, H_2O_2, and Cu ions were 5 wt%, 0.0025 mg mL^{-1}, 0.25 kU mL^{-1} and 0–75 μM, respectively. To form hydrogels, the solutions in the two microtubes were mixed (volume ratio = 1 : 1) together. The gelation time is determined by the vial-tilting method, which is defined as the time point when no flow is observed in the microtube.[21–23] The characteristics of GH hydrogels formed with different Cu^{2+} concentrations are listed in Table 1.

Rheological analysis of hydrogels

The mechanical strength (G') of GH/Cu hydrogels was determined using a rheometer (advanced rheometer GEM-150-050, Bohlin Instruments, Cranbury, NJ, USA) in an oscillation mode, with 0.01% strain (strain control), 0.1 Hz frequency, and using parallel-plate geometry (diameter = 25 mm, gap = 0.5 mm). On the bottom plate of the rheometer, we loaded 300 μL solution of hydrogel precursors prepared as described above. The upper plate was then immediately lowered down to the demanded gap. Then, the G' values of hydrogels were recorded continuously for 10 min at 37 °C.

Table 1 Characterization of GH/Cu hydrogels

Hydrogel	GH (wt%)	HRP (mg mL^{-1})	Tyr (kU mL^{-1})	H_2O_2 (wt%)	Cu^{2+} (μM)
GH	5	0.0025	0.25	0.02	0
GH/Cu25					25
GH/Cu50					50
GH/Cu75					75

Porous structure of hydrogels

The microporous structure of the GH/Cu hydrogels was investigated by field emission scanning electron microscopy (FE-SEM). Briefly, 600 μL of the hydrogels were prepared, followed by lyophilization to produce dried sponge-type hydrogels. The cross-sectional surfaces of the freeze-dried hydrogels were sputter-coated with gold, before observation by FE-SEM.

In vitro degradation

The *in vitro* enzymatic degradation rate of hydrogels was determined by using collagenase. 300 μL of different GH/Cu hydrogels was prepared in 1.5 mL microtubes. After equilibrating for 30 min, the initial weight of the hydrogel (W_i) was accurately recorded. Then, the hydrogels were incubated with 1 mL of PBS solution (0.01 M, pH 7.4) containing collagenase (0.001 wt%) at 37 °C. At predetermined time intervals, the media were removed, and the weight of the degraded hydrogels was recorded (W_t). After weighing, fresh media were added, and the hydrogels were continued to be incubated at 37 °C. The weight of the remaining hydrogel was calculated using the following equation:

$$\text{Weight of the remaining hydrogel (\%)} = W_d/W_i \times 100$$

In vitro release of copper ions from hydrogels

The amount of Cu ions released from GH/Cu hydrogels was determined using the copper assay Kit (Sigma-Aldrich, St. Louis, MO, USA USA). In brief, 300 μL of GH/Cu hydrogels were prepared in 1.5 mL microtubes and incubated in 1 mL of PBS at 37 °C with gentle shaking. At predetermined time points, the leachate buffer was completely withdrawn, and fresh buffer was replaced for the next interval. Then, the leachate buffer was incubated with master reaction mix supplied with the kit for 5 min at room temperature. The absorbances of blank (DIW), Cu ion standard, and leachate buffer were measured at 359 nm. Because Tyr is a copper-containing enzyme, the GH hydrogel prepared without Tyr is used as the control sample.

In situ biocatalytic generation of nitric oxide (NO) from hydrogels

The catalytic generation of NO from GH/Cu hydrogels was determined using the Saville–Griess reagent as described in previous studies.[24] The GH/Cu hydrogels were immersed in 1 mL of PBS (pH 7.4) solution containing NO donors (GSNO 10 μM and GSH 10 μM) and incubated at 37 °C in the dark with gentle shaking. At pre-determined time intervals, the medium was withdrawn and replaced with the fresh NO donor solution. To perform the Griess assay, 75 μL of the withdrawal medium was mixed with 75 μL of Griess solution (40 g L^{-1}) in the dark for 15 min. Then, the absorbance of the reacted solution was measured at 540 nm using a microplate spectrophotometer (Cytation™ 3 Cell Imaging Multi-Mode Reader, BioTek™, USA). The concentration of NO released from the GH/Cu hydrogel was calculated from the calibration curve constructed by using $NaNO_2$ at known concentrations (0–1 μM).

In vitro evaluation of anti-inflammatory properties

Human monocytic cells (THP-1) were cultured in RPMI-1640 media supplemented with 10% FBS and 1% PS in a humidified atmosphere with 5% CO_2 at 37 °C. Then, the cells at a density of 1×10^5 cells per mL were collected and cultured in RPMI-1640 media containing 200 ng mL^{-1} 12-myristate 13-acetate (PMA) for 2 days (d), followed by 1 d of PMA-free media to induce the differentiation of floating THP-1 into adherent M0 macrophages. 100 μL of GH/Cu hydrogels prepared in the insert system (Falcon® 24-well Insert Systems, PET Membrane, Corning, USA) were placed over the M0 cell layer and incubated in the culture media with or without the supplement of NO donors (10 μM GNSO and 10 μM GSH). As the positive control, M0 was incubated in RPMI-1640 media supplemented with 20 ng mL^{-1} IL-4 and 20 ng mL^{-1} IL-13 to induce the polarization into the M2 phenotype. After 48 h of incubation, the M2 polarization was evaluated by immunofluorescence staining (anti-CD163 antibody, ab87099, Abcam, Cambridge, UK) and enzyme-linked immunosorbent assay (TGF beta-1 ELISA Kit, BMS249-4, Invitrogen, California, USA), according to the manufacturer's protocol.

In vitro proliferation test using human umbilical vascular endothelial cells (HUVECs)

HUVECs were incubated the with CEFOgro-HUVEC medium containing growth factor supplements and 1% PS, in a humidified atmosphere with 5% CO_2 at 37 °C. The medium was changed everyday. After 3 d of incubation, HUVECs were harvested by trypsin–EDTA treatment and used for further testing.

For the proliferation test, 300 μL of the hydrogel was prepared as a thin layer on the bottom of the tissue culture plates (TCPs). After equilibrating for 30 min, HUVECs at a density of 1×10^4 cells per mL were seeded on the hydrogel layer and cultured in the media supplemented with or without NO donor solutions (10 μM GNSO and 10 μM GSH). It was noted that the NO donors were refreshed every 4 h. After 3 d of incubation, the unattached HUVECs were gently removed by rinsing with DPBS. Then, the proliferation of the attached HUVECs on the GH/Cu hydrogel was determined by WST-1 assay, according to the manufacturer's protocol. Briefly, the cells attached on the hydrogel were incubated with 1 mL of fresh culture media containing 10% WST-1 reagent at 37 °C. After 1 h, the absorbance of the reacted media was measured at 450 nm using a microplate spectrophotometer (Cytation™ 3 Cell Imaging Multi-Mode Reader, BioTek™, USA). In addition, the viability of the attached HUVECs was also investigated through live/dead staining assay. The cells were incubated with 1 mL of staining solution containing 2 mM calcein-AM and 4 mM ethidium homodimer-1, at 37 °C for 30 min, and the morphology of the adhered HUVECs was observed using a fluorescence microscope (Leica Microsystems, Korea).

In vitro HUVEC migration assay

The effect of GH/Cu hydrogels on the *in vitro* migration of HUVECs was investigated by the scratch test, as described in previous studies.[25,26] The HUVECs were seeded on the bottom of a 24-well plate at a density of 1×10^4 cells per mL and cultured at 37 °C in a 5% CO_2 atmosphere until the confluent monolayers formed. To create the wounds of similar sizes, a P200 pipette was used to scratch the cell layer in a straight line. After washing out the cell debris, the insert system containing 100 μL of the hydrogel was placed over the cell layer and fresh culture medium was added. The NO donors (10 μM GNSO and 10 μM GSH) were supplied every 4 h to ensure the sustained catalytic generation of NO. The change in size of the wounds was captured at predetermined time points and the migration rate of HUVECs was determined by using the equation:

$$\text{Wound closure} = (A_i - A_t)/A_i \times 100\%$$

where A_t is the wound area at time t and A_i is the initial wound area.

In vitro tube formation assay

The endothelial tube formation assay was performed using Corning® Matrigel® Matrix, according to the supplied protocol. Briefly, 100 μL of Matrigel solution was pre-coated on the TCPs to make a thin gel layer. The cells were then seeded on the Matrigel layer at a density of 1×10^5 cells per mL and incubated with CEFO culture media containing 5% FBS and 1% PS at 37 °C in a 5% CO_2 atmosphere for 1 d. Then, the insert system containing 100 μL of the hydrogel was placed over the cell layer and supplied with or without NO donors (10 μM GNSO and 10 μM GSH) for every 4 h. After 12 h of incubation, the formation of capillary-like structures on the Matrigel was recorded using an optical microscope. The length of the tube was calculated using the Image J program.

In ovo chicken chorioallantoic membrane (CAM) assay

The angiogenesis properties of GH/Cu were assessed by *in ovo* chicken chorioallantoic membrane (CAM) assay, following the previous studies.[27,28] First, the fertile eggs (Domestic, Korea) were incubated for 7 d (0–7 days) at 37–38 °C, 40–60% humidity and in the presence of O_2. During incubation, the eggs were rotated 90° every 12 h. On day 7 of incubation, the eggs were taken out and wiped with 70% alcohol. Then, a window of about 1 cm^2 was created on the eggshell to access the CAM underneath, and 100 μL of pre-formed GH/Cu hydrogel samples were carefully placed on the CAM of the embryo. The window was sealed by sterilized parafilm to prevent infection and incubated under aseptic conditions (37 °C, 40–60% humidity). On day 10, the images of the CAM-hydrogel complex representing the initial tissue response to biomaterials were taken using a digital camera. The Image J program was used to count the blood vessels around the hydrogels. All the experiments were performed under completely sterilized conditions in a laminar hood. The GH hydrogel loaded with 10 ng mL^{-1} of VEGF was used as the positive control and labeled as the VEGF sample.

In vivo subcutaneous injection of GH/Cu hydrogels

All the animal experiments in this study were conducted in strict accordance with a high standard guideline approved by

the Incheon National University Institutional Animal Care and Use Committee (INU-ANIM-2021-08). The study was divided into five experimental groups (VEGF, GH, GH/Cu25, GH/Cu50, and GH/Cu75). Briefly, under anesthesia, 100 μL of hydrogel samples were subcutaneously injected into the dorsal region of the mice (n = 5 for each group). After three weeks, the mice were sacrificed to collect the subcutaneous tissue containing hydrogel samples. The collected tissues were immediately fixed in 4% paraformaldehyde for 1 d, followed by paraffin embedding and sectioning. The tissue sections were subjected to histological analysis using hematoxylin and eosin (H&E) staining and immunohistochemical analysis using the anti-alpha smooth muscle actin antibody (anti-αSMA, ab5694, Abcam, Cambridge, UK) and the anti-vascular endothelial growth factor A antibody (anti-VEGFA, ab1316, Abcam, Cambridge, UK), following the manufacturer's protocol.

Statistical analyses

All experiments were repeated at least three times, and each condition was analyzed in triplicate. The data are analyzed using one-way ANOVA followed by the t-test and are presented as mean ± standard deviation. $P < 0.05$ was considered statistically significant.

Results and discussion

Hydrogel formation

Gelatin is a biodegradable natural polymer with excellent biocompatibility and has been widely used as an ideal hydrogel candidate. Containing a large number of amino and carboxyl groups, gelatin can be easily functionalized with various target moieties, such as phenol, thiol, and methacrylate. In addition, gelatin brings many benefits to biomedical applications with its biodegradability in physiological environments. We previously reported the use of phenol-rich gelatin to prepare injectable hydrogels by the enzymatic catalysis of HRP/H_2O_2 for various biomedical applications.[22,24,29–31] In these studies, the GH polymer was synthesized through the amide bonds between the carboxyl groups of HPA and amine groups of gelatin. After that, in the presence of H_2O_2, HRP oxidized phenols into phenol radicals, enabling the crosslinking of the aromatic ring by C–C or C–O coupling.[32,33] By adjusting the phenol contents of GH or varying the concentration of HRP and H_2O_2 during the gelation, the physicochemical properties of the resulting hydrogels were easily controlled, which showed the potential for various biomedical applications, such as drug/cell delivery,[34,35] wound healing,[30,36] and cancer treatment. In this study, we prepare the copper nanoparticle encapsulated GH hydrogel (GH/Cu) under the catalysis of dual enzymatic activities of HRP and Tyr (Fig. 1), to create a multifunctional NO-releasing hydrogel. Herein, Tyr is a well-known metalloenzyme that contains two copper ions in the active site.[37] Tyr can oxidize the hydroxyl group of phenol into *ortho*-quinones and catechol, and *ortho*-quinones with high electrophilicity can participate in many reactions, including Michael-type addition, Schiff-base reaction, and coupling reaction. Meanwhile, catechol groups present in the aerobic environment provide (1) activated target moieties for crosslinking reaction between GH hydrogel precursors and (2) binding sites for the *in situ* formation of CuNPs that catalyze NO generation.[22,38]

Gelation time, mechanical properties, degradation rates, and porous structures of hydrogels

The gelation time is a crucial parameter affecting the intended applications of hydrogels, because too rapid gelation causes

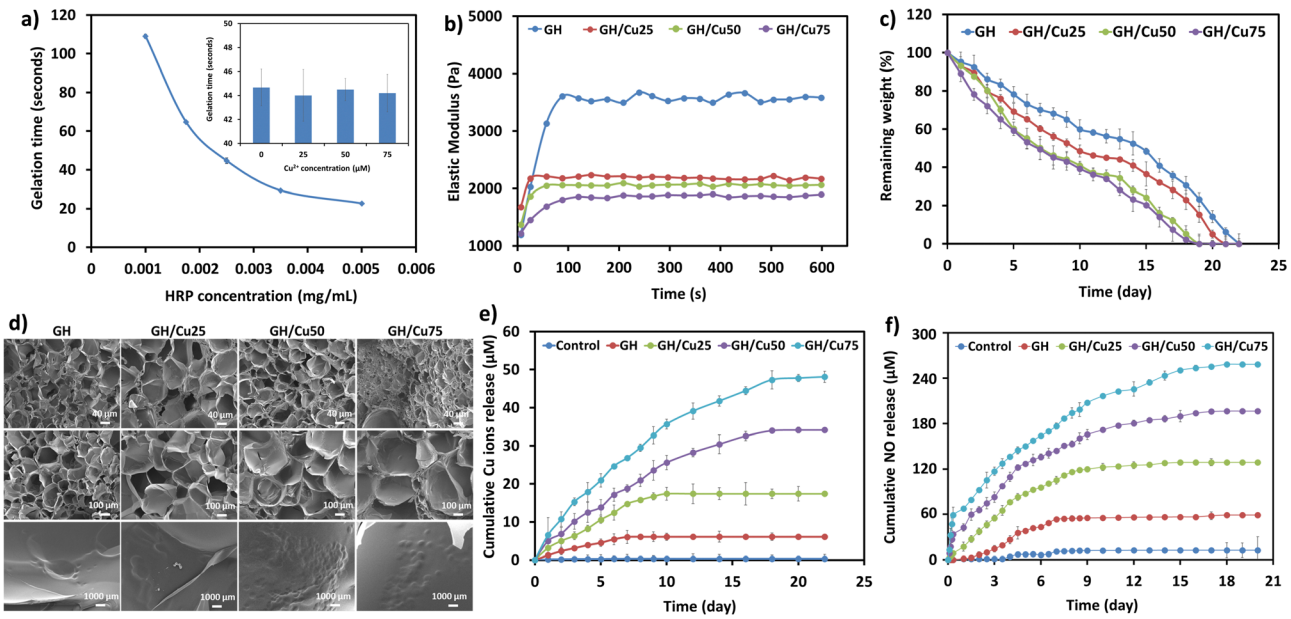

Fig. 2 Characterization of the GH/Cu hydrogel. (a) Gelation time defined by the vial titling method as a function of HRP concentration and copper ion concentration (inset figure), (b) mechanical strength evaluated using a rheometer, (c) degradation rate in lysozyme, (d) cross-sectional morphology under the SEM, (e) cumulative copper ions released from GH/Cu hydrogels after incubation in PBS, and (f) cumulative NO release by incubating the GH/Cu hydrogel in the presence of 10 μM GSNO and 10 μM GSH as NO donors. Data are presented as means ± SD ($n \geq 3$) and analyzed using one-way ANOVA.

difficulty during injection or is insufficient to fulfill the irregular shape of the defect. In contrast, slow gelation will result in the leakage of the hydrogel precursors and encapsulated materials during the gelation process *in vivo*.[39] Generally, the gelation time of enzymatically crosslinked hydrogels is readily controlled by varying enzyme concentration.[24,30,39] Previously, we reported that the addition of Tyr (0.25 kU mL^{-1}) did not affect the gelation rate, while significantly improving the adhesive strength of the HRP-crosslinked hydrogel.[22] Therefore, in this study, we investigated the effect of HRP on the gelation time of the GH/Cu hydrogel by fixing the concentrations of GH polymer (5 wt%), H_2O_2 (0.02 wt%), Tyr (0.25 kU mL^{-1}), and Cu^{2+} (25 μM). Fig. 2a illustrates that increasing HRP concentration from 0.001 to 0.005 mg mL^{-1} shortened the gelation time from around 110 s to 20 s. This result is in agreement with previous studies, which demonstrated the rapid and controllable gelation time of hydrogels crosslinked by HRP.[21,22,24,31,39,40] Moreover, the effect of the addition of Cu^{2+} on the gelation rate of the hydrogel was unremarkable (inset of Fig. 2a).

It is noted that during the gelation process, Cu^{2+} ions interact with catechol moieties for the *in situ* formation of Cu NPs, leading to the remarkable change in the hydrogel's structure. Therefore, we investigated the effect of embedded Cu NPs on other physicochemical properties of the resulting GH/Cu hydrogels, including elastic modulus, tissue adhesiveness, degradation rate, and porosity.

As shown in Fig. 2b, the elastic moduli (G' value) of GH hydrogels dramatically dropped from 3600 Pa to ~2000 Pa with increasing Cu^{2+} concentration. In fact, the hydrogel without Cu^{2+} addition (GH) showed the highest G' value (3600 Pa), followed by GH/Cu25 (2100 Pa), GH/Cu50 (2000 Pa), and GH/Cu75 (1850 Pa). The decrease in the elastic moduli of GH/Cu hydrogels can be explained by the competition between phenol–phenol oxidative coupling and the phenol–metal coordinative coupling reaction. During the gelation process, Tyr converts phenol groups into catechol groups, subsequently forming the copper–catechol complexes within the hydrogel matrix. Compared to the HRP-inducing phenol–phenol covalent bond, this metal-coordination occurred more rapidly with lower strength.[41,42] Therefore, at the fixed concentrations of HRP and Tyr, the mechanical strength of GH hydrogels tends to decrease with the increase of Cu^{2+} concentration. Moreover, the impact of Cu^{2+} concentration on the adhesive and tensile strengths of the hydrogels was investigated, as shown in Fig. S1 (ESI†). The results reveal a significant improvement in adhesive strength for all GH and GH/Cu hydrogels in comparison to fibrin glue, which is attributed to the additional interactions between hydrogels and nucleophiles on tissue surfaces as discussed previously.[22] Conversely, tensile strength exhibited a slight decrease with the introduction of Cu^{2+}, aligning with the elastic modulus but without notable variation across different Cu^{2+} concentrations in the hydrogel. The reduced mechanical strength also results in a faster degradation rate and larger pore size of GH/Cu hydrogels, compared to the pure GH hydrogel (Fig. 2c and d). The successful *in situ* formation of Cu NPs within the GH hydrogel matrix was also characterized and observed by SEM and TEM. As shown in Fig. 2d and Fig. S2 (ESI†), most particles were spherical and uniform with an average diameter of 20 ± 3.92 nm. In addition, a higher amount of particles were found as the concentration of Cu^{2+} ions increased during the gelation process.

Controlled release of Cu ions for catalytic NO generation

Copper ions are well-known catalysts for the decomposition of *S*-nitrosothiols (RSNOs). During this process, Cu^{2+} is reduced to Cu^{+} in the presence of thiol (RSH), triggering the generation of NO.[43–46] Compared with other approaches using finite reservoirs of NO donor molecules (*e.g.*, *S*-nitrosoglutathione, *N*-diazeniumdiolates, and *S*-nitroso-*N*-acetylpenicillamine), the use of NO catalysts, such as metal ions or organoselenium, has potential advantages.[47–49] Different from the decomposition of NO donor molecules triggered by heat, light, pH, or moisture, metal ions catalyze the *in situ* generation of NO upon contact with available RSNO sources within the biological system, leading to the continuous delivery of NO for extended periods.[50] In addition, because metal ions are also more stable than NO donor molecules, the incorporation of metal ions into the carrier can be easily performed, without affecting their activities. The release of NO from endogenous RSNOs through the catalytic activity of Cu ions is described by the following scheme:

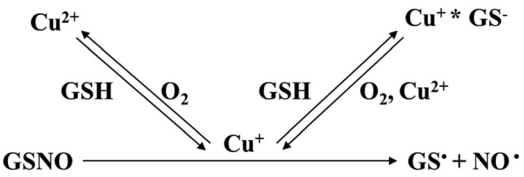

The scheme shows that the NO release would be directly affected by the release amount of Cu ions from GH/Cu hydrogels. As shown in Fig. 2e, there was a small amount of Cu ions (6.03 μM) released from GH within the first week, due to the degradation of Tyr (copper-containing enzyme). The GH/Cu hydrogels showed a prolonged-release time and higher Cu ion release amount, depending on the concentration of embedded Cu. For example, Cu ions were sustained released within 10, 20, and 21 d from GH/Cu25, GH/Cu50, and GH/Cu75, respectively. In addition, GH/Cu75 exhibited the highest accumulative concentration of Cu at about 47.08 μM, compared to GH/Cu50 and GH/Cu25 (34.13 and 17.39 μM, respectively). Importantly, the amount of Cu ions released per day from all GH/Cu hydrogels is in the range of normal serum concentration of copper (10–25 μM), which does not cause cytotoxicity toward mammalian cells.[51]

Next, the NO release profile from GH/Cu hydrogels in the presence of NO donors (10 μM GSNO and 10 μM GSH) was evaluated by Griess assay. As shown in Fig. 2f, the control sample (the GH hydrogel formed in the absence of Tyr) and GH hydrogel release a trivial amount of NO, which is attributed to the self-decomposition of the NO donor at 37 °C and the presence of Cu-containing Tyr, respectively. In contrast, the

release of NO from GH/Cu hydrogels was significantly increased, correlated with the release amount of Cu ions. For example, the amounts of NO released were up to 115 μM, 142 μM, and 180 μM for GH/Cu25, GH/Cu50, and GH/Cu75 after 7 d, respectively. Moreover, the NO release from GH/Cu hydrogels was prolonged up to 21 d, depending on the release behaviour of Cu ions. These results indicated the controllable and prolonged NO release of our GH/Cu hydrogel system, by simply varying the feeding concentrations of Cu^{2+} during the gelation process, which would be applied for various wounds (*e.g.*, infectious wounds, chronic wounds, diabetic ulcer).

In vitro anti-inflammatory properties of GH/Cu hydrogels

The immediate activation of the immune system after injury provokes a local inflammatory response. This inflammatory response plays crucial roles in both normal and pathological wound healing. It is well documented that inflammatory reaction is essential to fight against the pathogen and remove the dead cell/tissue from the injured site. However, prolonged inflammation leads to delayed tissue formation and remodelling phase in wound healing.[52] Therefore, shortening the inflammation phase is considered as an effective strategy to promote the healing process. During inflammation, macrophages are recruited from the circulation and are classified into the M1 pro-inflammatory or M2 anti-inflammatory phenotype. Unlike the M1 phenotype, the M2 phenotype stimulates the production of anti-inflammatory factors (*e.g.*, IL-4, IL-10, and TGF-β) and modulates the tissue repair.[53,54] The polarization of macrophages into the M2 phenotype has been demonstrated to be an efficient approach to control and hasten the inflammation phase. Herein, we evaluated the anti-inflammatory activities of GH/Cu hydrogels through the effect of NO release on inducing the polarization of macrophages into the M2 phenotype.[55,56] The expression of surface marker CD163 and the secretion of TGF-β cytokine were investigated to confirm the M2 phenotype polarization stimulated by GH/Cu hydrogels.[57]

As shown in Fig. 3a, the nuclei of all cell types were stained with blue fluorescence, while only CD163-expressing M2 macrophages were stained with green fluorescence. Interestingly, in the presence of NO donors, the strong intensity of green fluorescence was clearly observed on GH/Cu-treated macrophages, comparable with the M2 positive control sample. The CD163 intensity increased with the increase in the amount of NO generated from GH/Cu25, GH/Cu50, and GH/Cu75 (Fig. 3b). In addition, the amount of TGF-β released from the GH/Cu-treated macrophages was also significantly higher than those released from the M0 control and GH-treated macrophages. In detail, 23.37, 32.09, and 44.85 pg mL^{-1} TGF-β were released from GH/Cu25, GH/Cu50, and GH/Cu75 treated macrophages in the presence of NO donors, respectively (Fig. 3c). These results confirm the effect of NO released from the GH/Cu

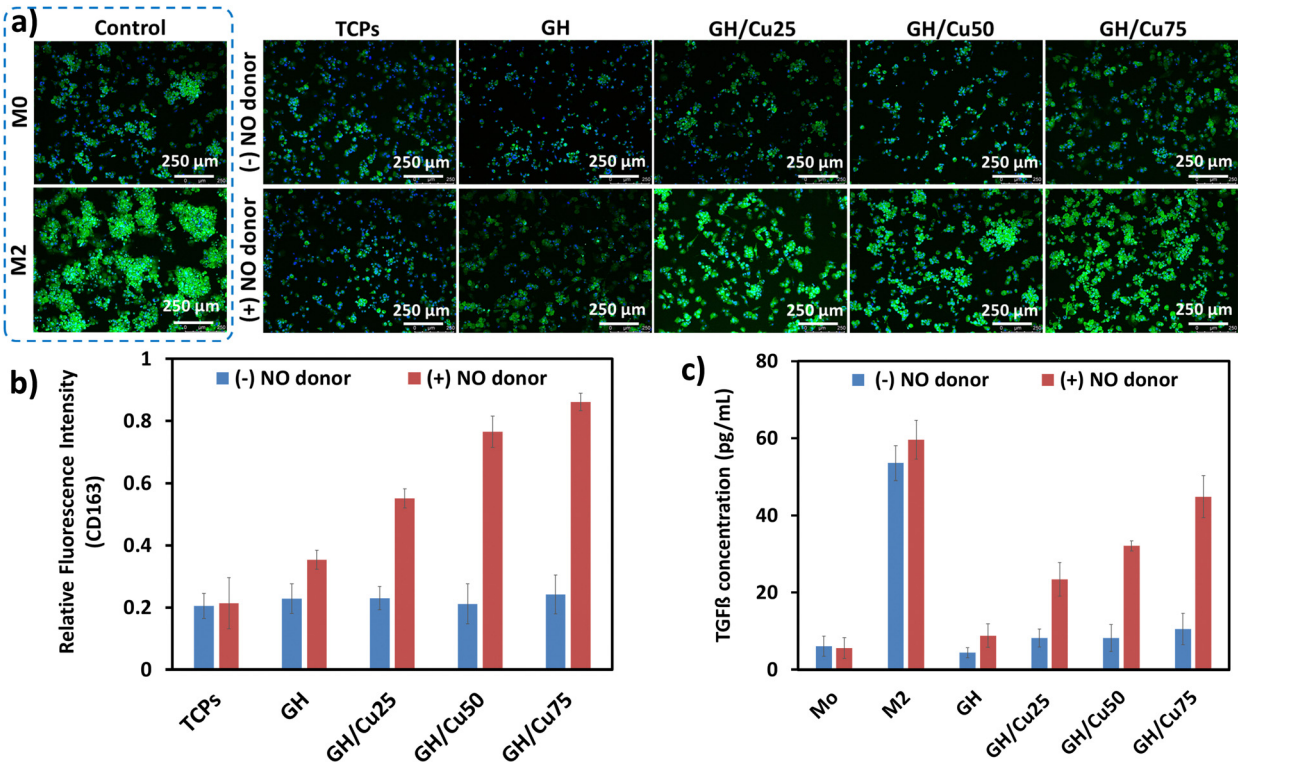

Fig. 3 *In vitro* anti-inflammatory properties. (a) Immunofluorescence staining images of adhered macrophages with DAPI (blue) and CD163 (green), (b) quantification of the relative average fluorescence intensity of CD163 compared to the M2 macrophage control group, and (c) concentration of TGF-ß released from macrophages by ELISA. Data are presented as means ± SD ($n \geq 3$) and analyzed using one-way ANOVA, $^{**}p < 0.01$, $^{***}p < 0.001$ *versus* the TCPs and M2 sample, respectively.

hydrogel on increasing anti-inflammatory M2 gene expression, which likely contributes to the higher wound healing efficiency.

In vitro angiogenic activity of the GH/Cu hydrogel toward HUVECs

NO is widely known to be a vasodilator that can stimulate EC growth and migration, thus encouraging new vessels to sprout from existing ones.[28,58] We firstly determined the effect of NO release from GH/Cu hydrogels on the proliferation and migration of HUVECs. The viability of HUVECs cultured on GH and GH/Cu hydrogels was investigated through live/dead staining and WST-1 assay. Due to the intrinsic nature of the ECM,[59] all gelatin-based GH and GH/Cu hydrogels showed excellent cytocompatibility toward HUVECs, represented by the high number of green-stained cells (Fig. 4a). Moreover, the higher amount of NO released from GH/Cu in the presence of NO donors resulted in the better attachment and well spreading of cells on the hydrogels. As presented in Fig. 4b, all the GH/Cu samples showed the impressive growth of HUVECs by almost two times under NO donor supply, compared with TCPs. These results could confirm the cytocompatibility of the GH/Cu hydrogel system for further *in vitro* and *in vivo* experiments.

Next, we determined the impact of the NO-releasing hydrogel on the migration rate of HUVECs, using scratch assay. Fig. 4c and d indicate that GH/Cu could induce faster migration of HUVECs in an NO concentration-dependent manner. Without the release of NO from hydrogel samples, the cells migrated slowly, and after 24 h, below 50% of the collective scratch area was closed. In the presence of NO donors, GH/Cu25, GH/Cu50, and GH/Cu75 promoted HUVEC migration, which covered 43, 52, and 60% of the collective scratch area, respectively, after 12 h, and completely healed the scratches within 24 h of incubation. These results verify the effect of continuous and controlled NO releasing hydrogels on accelerating endothelial cell proliferation and migration, which are critical events for angiogenesis in the wound healing process.

In vitro tube formation assay is one of the most rapid and simple models to mimic the *in vivo* angiogenesis, which is used to evaluate the angiogenic properties of NO-releasing hydrogels. As we expected, no hydrogel-treated samples clearly showed the alignment of cells in the capillary tube in the absence of NO donors, excepting VEGF control (Fig. 5a and b). Meanwhile, with the addition of GSNO and GSH, the catalytic generation of NO from GH/Cu hydrogels is induced, resulting in the stimulation of capillary tube formation. While GH and GH/Cu25 only presented a moderate stimulation effect on the sprouting and connection of HUVECs to form the tube, GH/Cu50 and GH/Cu75 significantly promoted the formation of a clearly tubular network with a greater number of nodes and branches, as well as longer branches. In particular, GH/Cu50 and GH/Cu75 exhibited around 90% efficiency compared with VEGF treatment. These findings are consistent with previous studies, demonstrating the effect of NO on the behaviour of endothelial cells during angiogenesis, including enhanced proliferation, a faster migration rate, and improved tube formation.[28,58,60]

In ovo chicken chorioallantoic membrane (CAM) assay

We hypothesized that GH/Cu hydrogels would induce the *in situ* formation of NO, therefore facilitating the neovascularization *in vivo*.[60,61] To confirm this hypothesis, we performed CAM assay, a simple, easily accessible, and cost-effective model for the evaluation of angiogenic activity of biomaterials in tissue engineering. When implanting hydrogel samples for 3 d, many new blood vessels grew around the VEGF-encapsulated hydrogel (positive control) on the CAM (Fig. 6a). Compared to the control group, there was no difference in the

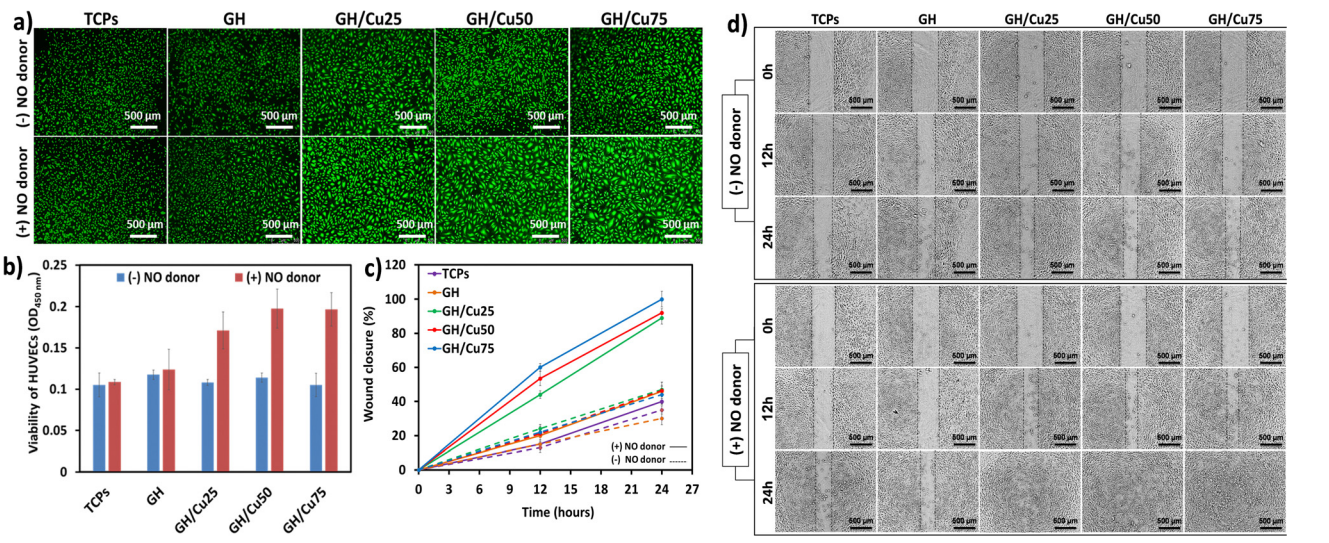

Fig. 4 *In vitro* angiogenic activities of GH/Cu hydrogels: (a) live (green)/dead (red) staining, (b) viability of HUVECs after being cultured with hydrogel samples for 3 d by WST-1 assay, (c) quantification of the migration rate and (d) optical microscopy images showing the migration of HUVECs using wound scratch migration assay. Data are presented as means ± SD ($n \geq 3$), and analyzed using one-way ANOVA, $^{**}p < 0.01$, $^{***}p < 0.001$ *versus* the control sample.

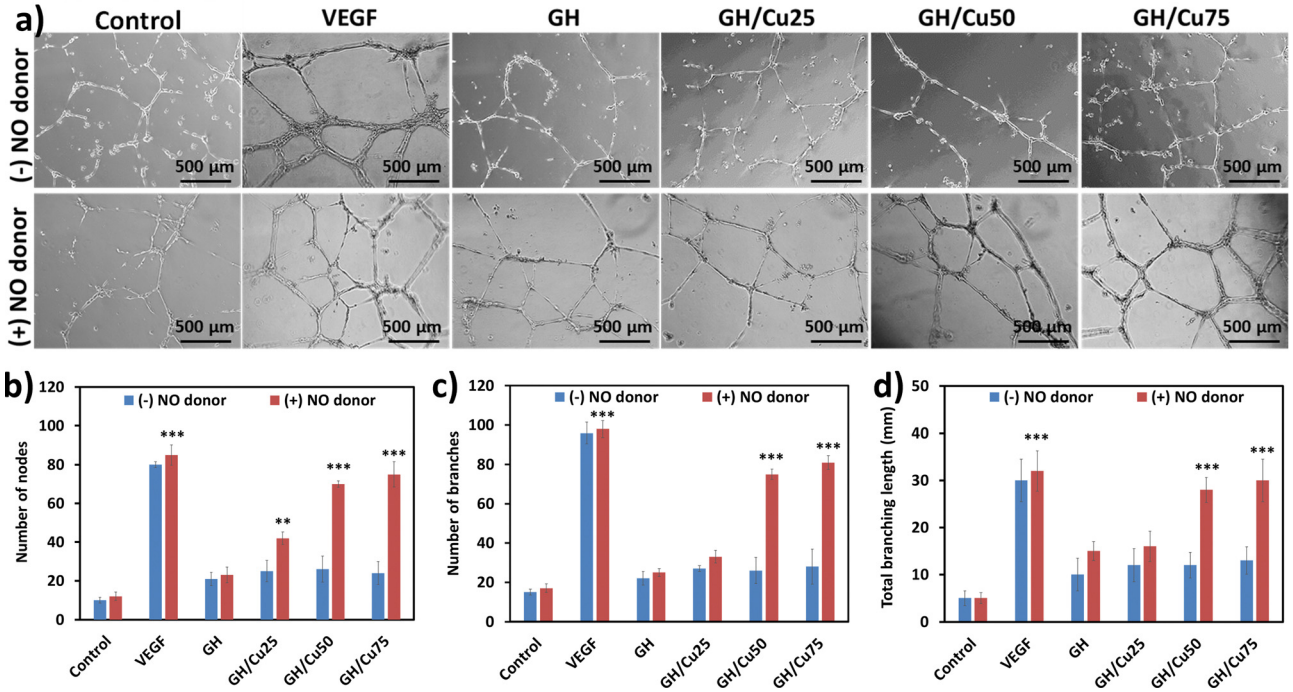

Fig. 5 Angiogenic activity evaluated by *in vitro* endothelial tube formation assay: (a) optical microscopy images showing the formation of the cellular network and quantitative evaluation of various parameters, including (b) the number of nodes, (c) the number of branches, and (d) the total branching length. Data are presented as means ± SD ($n \geq 3$) and analyzed using one-way ANOVA.

CAM after incubating with GH and GH/Cu25, while GH/Cu50 and GH/Cu75 stimulated the growth of many new blood vessels. This result indicates that GH/Cu hydrogels supply sufficient NO to induce new blood vessel formation in the *in*

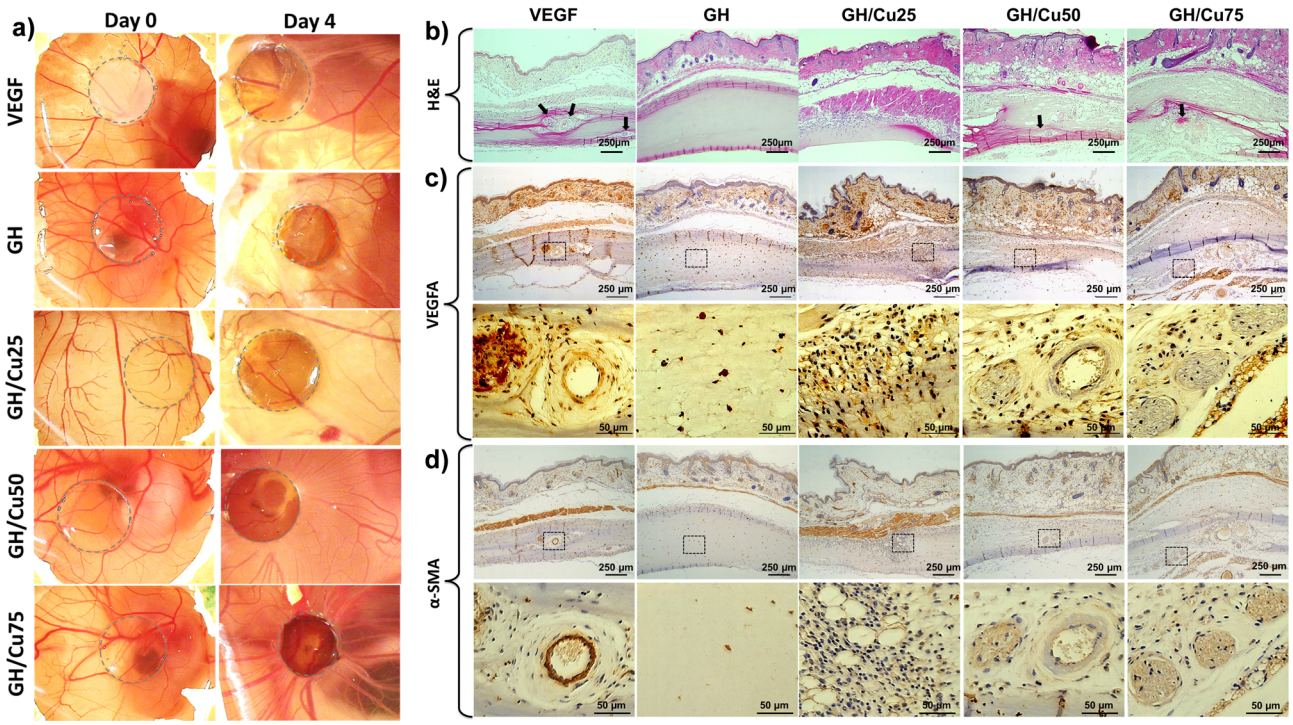

Fig. 6 (a) Angiogenic activity evaluated from the optical image of new blood vessel formation in *in ovo* chicken chorioallantoic membrane angiogenesis (CAM) assay. Angiogenic activity evaluated by *in vivo* subcutaneous injection of the hydrogel. (b) Histological H&E staining and immunobiological staining with (c) the VEGFA antibody (purple: nucleus, brown: VEGFA), and (d) α-SMA to stain the smooth muscle cells (purple: nucleus, brown: α-SMA).

ovo model, which offers potential for use in further animal studies.[58,61–64]

In vivo subcutaneous injection of GH/Cu hydrogels

During tissue remodelling, new blood vessel formation is essential to facilitate the wound healing rate. Thus, the degree of neovascularization by hydrogels in these processes was investigated *in vivo* through H&E and immunohistochemical staining. From the H&E staining, it was found that the GH group did not show any signal of cell infiltration; meanwhile, other groups, including VEGF, GH/Cu25, GH/Cu50, and GH/Cu75, presented moderate cell infiltration. Moreover, new blood vessels were also observed in these groups (Fig. 6b, arrowheads). These results were further confirmed by immunohistochemical staining of α-SMA and VEGFA.

The intima layer and media layer of all vessels are composed of endothelial cells and smooth muscle cells, respectively. Vascular endothelial growth factor A (VEGF-A) is considered to be the essential, dominant inducer of the growth of blood vessels by promoting the growth and migration of endothelial cells. On the other hand, during the differentiation of smooth muscle cells in the vessel wall, the α-smooth-muscle actin was strongly expressed and became a marker for this process. Therefore, VEGFA and α-SMA staining was used to illustrate the cross-section of blood vessels inside the VEGF, GH/Cu50, and GH/Cu75 hydrogels (Fig. 6c and d). Similar to the results obtained from H&E staining, the GH hydrogel did not show any penetration of cells into the hydrogel. Meanwhile, inside the GH/Cu25 hydrogel, a high number of penetrated cells preparing for the early stage of vessel formation were observed. Better than GH/Cu25, many new vessels were found at both the margin and interior area of the VEGF, GH/Cu50, and GH/Cu75 hydrogels. While the vessels inside the VEGF hydrogel were defined by the clearly and completely formed circles, GH/Cu50 and GH/Cu75 promote the formation of new vessels at an early stage. Taken together, these results show that the considerable amount of NO released from GH/Cu50 and GH/Cu75 has the potency to promote angiogenesis and enhance cell remodelling in the animal model. Lastly but importantly, all mice are alive after three weeks of subcutaneous injection of hydrogel samples, revealing that GH/Cu hydrogels are non-toxic in nature and readily safe for *in vivo* administration.

Conclusion

In this study, we successfully developed injectable NO-releasing gelatin-based hydrogels (GH/Cu) as potential wound dressing materials, by simply embedding the copper ions as the NO-generating catalyst in the hydrogel systems. The hydrogels were fabricated from a phenol-containing gelatin polymer (GH) through a dual-enzymatic catalysis of HRP and Tyr. The NO release behaviors of hydrogels were easily controlled by varying the concentration of copper ions, without compromising the cytocompatibility of hydrogels. We found that the release of NO from GH/Cu hydrogels remarkably enhanced the expression of the M2 anti-inflammatory macrophage and promoted the proliferation and migration of HUVECs. The angiogenic activities of these hydrogels were also demonstrated through the stimulation of *in vitro* tube formation using HUVECs and *in ovo* new blood vessel formation in the CAM. In addition, our hydrogels allowed the penetration of cells and showed signals of the early stage of new vessel formation upon *in vivo* subcutaneous injection. Taken together, we believe that our GH/Cu hydrogels could be used as advanced materials for both wound treatment and other biomedical applications related to angiogenesis and inflammation response. However, the *in vivo* enhanced wound healing ability of GH/Cu hydrogels should be investigated in acute/chronic wound models, to thoroughly evaluate the synergistic effect of bioactive hydrogels and NO release on promoting whole-process wound healing.

Conflicts of interest

There are no conflicts to declare.

Acknowledgements

This work was supported by the Priority Research Centers Program (2019R1A6A1A11051471) funded by the National Research Foundation of Korea (NRF) and by the Alchemist Project of the Korea Evaluation Institute of Industrial Technology (KEIT 20018560, NTIS 1415184668) funded by the Ministry of Trade, Industry & Energy (MOTIE, Korea).

Notes and references

1 H. Brem, M. Tomic-Canic, A. Tarnovskaya, H. P. Ehrlich, E. Baskin-Bey, K. Gill, M. Carasa, S. Weinberger, H. Entero and B. Vladeck, *Surg. Technol. Int.*, 2003, **11**, 161–167.
2 M. A. Gershater and J. Apelqvist, *Expert Rev. Pharmacoecon. Outcomes Res.*, 2021, **21**, 277–284.
3 S. Dhivya, V. V. Padma and E. Santhini, *Biomedicine*, 2015, **5**, 22.
4 A. Stejskalova and B. D. Almquist, *Biomater. Sci.*, 2017, **5**, 1421–1434.
5 P. Wang, S. Jiang, Y. Li, Q. Luo, J. Lin, L. Hu, X. Liu and F. Xue, *Nanomedicine*, 2021, **34**, 102381.
6 L. H. Dang, T. H. Nguyen, H. L. B. Tran, V. N. Doan and N. Q. Tran, *J. Healthcare Eng.*, 2018, **2018**, 5754890.
7 C. Ghobril and M. W. Grinstaff, *Chem. Soc. Rev.*, 2015, **44**, 1820–1835.
8 X. Zhao, H. Wu, B. Guo, R. Dong, Y. Qiu and P. X. Ma, *Biomaterials*, 2017, **122**, 34–47.
9 Z. He, Q. Xu, B. Newland, R. Foley, I. Lara-Saez, J. F. Curtin and W. Wang, *J. Mater. Chem. B*, 2021, **9**, 6326–6346.
10 S. Barrientos, O. Stojadinovic, M. S. Golinko, H. Brem and M. Tomic-Canic, *Wound Repair Regen.*, 2008, **16**, 585–601.
11 S. Guo and L. A. Dipietro, *J. Dent. Res.*, 2010, **89**, 219–229.

12 R. Ahmed, R. Augustine, M. Chaudhry, U. A. Akhtar, A. A. Zahid, M. Tariq, M. Falahati, I. S. Ahmad and A. Hasan, *Biomed. Pharmacother.*, 2022, **149**, 112707.
13 M. Kandhwal, T. Behl, A. Kumar and S. Arora, *Curr. Pharm. Des.*, 2021, **27**, 1999–2014.
14 M. Wu, Z. Lu, K. Wu, C. Nam, L. Zhang and J. Guo, *J. Mater. Chem. B*, 2021, **9**, 7063–7075.
15 M. J. Malone-Povolny, S. E. Maloney and M. H. Schoenfisch, *Adv. Healthcare Mater.*, 2019, **8**, e1801210.
16 B. B. Childress and J. K. Stechmiller, *Biol. Res. Nurs.*, 2002, **4**, 5–15.
17 P. Abaffy, S. Tomankova, R. Naraine, M. Kubista and R. Sindelka, *BMC Genomics*, 2019, **20**, 815.
18 J. D. Luo and A. F. Chen, *Acta Pharmacol. Sin.*, 2005, **26**, 259–264.
19 C. La Torre, B. Cinque, F. Lombardi, G. Miconi, P. Palumbo, Z. Evtoski, G. Placidi, D. Fanini, A. M. Cimini, E. Benedetti, M. Giuliani and M. G. Cifone, *J. Cell. Physiol.*, 2016, **231**, 2185–2195.
20 G. Tavares, P. Alves and P. Simoes, *Pharmaceutics*, 2022, **14**(7), 1377.
21 Y. Lee, J. W. Bae, D. H. Oh, K. M. Park, Y. W. Chun, H. J. Sung and K. D. Park, *J. Mater. Chem. B*, 2013, **1**, 2407–2414.
22 P. Le Thi, Y. Lee, D. H. Nguyen and K. D. Park, *J. Mater. Chem. B*, 2017, **5**, 757–764.
23 K. M. Park, Y. Lee, J. Y. Son, D. H. Oh, J. S. Lee and K. D. Park, *Biomacromolecules*, 2012, **13**, 604–611.
24 T. T. Hoang Thi, Y. Lee, P. Le Thi and K. D. Park, *Acta Biomater.*, 2018, **67**, 66–78.
25 D. L. Tran, P. Le Thi, S. M. Lee, T. T. Hoang Thi and K. D. Park, *J. Controlled Release*, 2020, **329**, 401–412.
26 C. C. Liang, A. Y. Park and J. L. Guan, *Nat. Protoc.*, 2007, **2**, 329–333.
27 Z. Li, T. Qu, C. Ding, C. Ma, H. Sun, S. Li and X. Liu, *Acta Biomater.*, 2015, **13**, 88–100.
28 F. Kabirian, P. Brouki Milan, A. Zamanian, R. Heying and M. Mozafari, *Acta Biomater.*, 2019, **92**, 82–91.
29 D. H. Choi, K. E. Lee, S. Y. Oh, S. M. Lee, B. S. Jo, J. Y. Lee, J. C. Park, Y. J. Park, K. D. Park, I. Jo and Y. S. Park, *Biomaterials*, 2021, **278**, 121156.
30 P. L. Thi, Y. Lee, D. L. Tran, T. T. H. Thi, J. I. Kang, K. M. Park and K. D. Park, *Acta Biomater.*, 2020, **103**, 142–152.
31 Y. Lee, K. H. Choi, K. M. Park, J. M. Lee, B. J. Park and K. D. Park, *ACS Appl. Mater. Interfaces*, 2017, **9**, 16890–16899.
32 G. R. Lopes, D. C. G. A. Pinto and A. M. S. Silva, *RSC Adv.*, 2014, **4**, 37244–37265.
33 M. Khanmohammadi, M. B. Dastjerdi, A. Ai, A. Ahmadi, A. Godarzi, A. Rahimi and J. Ai, *Biomater. Sci.*, 2018, **6**, 1286–1298.
34 Y. Lee, J. W. Bae, J. W. Lee, W. Suh and K. D. Park, *J. Mater. Chem. B*, 2014, **2**, 7712–7718.
35 S. H. Lee, Y. Lee, Y. W. Chun, S. W. Crowder, P. P. Young, K. D. Park and H. J. Sung, *Adv. Funct. Mater.*, 2014, **24**, 6771–6781.
36 D. S. Yoon, Y. Lee, H. A. Ryu, Y. Jang, K. M. Lee, Y. Choi, W. J. Choi, M. Lee, K. M. Park, K. D. Park and J. W. Lee, *Acta Biomater.*, 2016, **38**, 59–68.
37 S. Choi, H. Ahn and S. H. Kim, *J. Appl. Polym. Sci.*, 2022, **138**(14), 51887.
38 E. Solem, F. Tuczek and H. Decker, *Angew. Chem., Int. Ed.*, 2016, **55**, 2884–2888.
39 J. W. Bae, J. H. Choi, Y. Lee and K. D. Park, *J. Tissue Eng. Regener. Med.*, 2015, **9**, 1225–1232.
40 D. L. Tran, P. Le Thi, T. T. Hoang Thi and K. D. Park, *Prog. Nat. Sci.: Mater. Int.*, 2020, **30**, 661–668.
41 Z. Xu, *Sci. Rep.*, 2013, **3**, 2914.
42 J. Yang, M. A. C. Stuart and M. Kamperman, *Chem. Soc. Rev.*, 2014, **43**, 8271–8298.
43 A. C. Gorren, A. Schrammel, K. Schmidt and B. Mayer, *Arch. Biochem. Biophys.*, 1996, **330**, 219–228.
44 D. J. Barnett, J. McAninly and D. L. H. Williams, *J. Chem. Soc., Perkin Trans. 2*, 1995, **2**(4), 741–745.
45 A. P. Dicks, H. R. Swift, D. L. H. Williams, A. R. Butler, H. H. Al-Sa'doni and B. G. Cox, *J. Chem. Soc., Perkin Trans. 2*, 1996, (4), 481–487.
46 Helen R. Swift and D. Lyn H. Williams, *J. Chem. Soc., Perkin Trans. 2*, 1997, 1933–1935.
47 A. B. Seabra, G. Z. Justo and P. S. Haddad, *Biotechnol. Adv.*, 2015, **33**, 1370–1379.
48 H. Yu, L. X. Cui, N. Huang and Z. L. Yang, *Med. Gas Res.*, 2019, **9**, 184–191.
49 X. Zhou, J. Zhang, G. Feng, J. Shen, D. Kong and Q. Zhao, *Curr. Med. Chem.*, 2016, **23**, 2579–2601.
50 J. Rao, H. Pan Bei, Y. Yang, Y. Liu, H. Lin and X. Zhao, *Front. Bioeng. Biotechnol.*, 2020, **8**, 578.
51 National Academies of Sciences, Engineering, and Medicine, Dietary Reference Intakes for Thiamin, Riboflavin, Niacin, Vitamin B6, Folate, Vitamin B12, Pantothenic Acid, Biotin, and Choline. Washington, DC: The National Academies Press, 1998, DOI: 10.17226/6015.
52 S. K. Shukla, A. K. Sharma, V. Gupta and M. H. Yashavarddhan, *J. Tissue Viability*, 2019, **28**, 218–222.
53 K. L. Spiller, R. R. Anfang, K. J. Spiller, J. Ng, K. R. Nakazawa, J. W. Daulton and G. Vunjak-Novakovic, *Biomaterials*, 2014, **35**, 4477–4488.
54 D. Torre, R. Tambini, S. Aristodemo, G. Gavazzeni, A. Goglio, C. Cantamessa, A. Pugliese and G. Biondi, *Mediators Inflammation*, 2000, **9**, 193–195.
55 D. Tang, S. Chen, D. Hou, J. Gao, L. Jiang, J. Shi, Q. Liang, D. Kong and S. Wang, *Mater. Sci. Eng., C*, 2018, **84**, 1–11.
56 W. J. Lee, S. Tateya, A. M. Cheng, N. Rizzo-DeLeon, N. F. Wang, P. Handa, C. L. Wilson, A. W. Clowes, I. R. Sweet, K. Bomsztyk, M. W. Schwartz and F. Kim, *Diabetes*, 2015, **64**, 2836–2846.
57 S. Kadomoto, K. Izumi and A. Mizokami, *Int. J. Mol. Sci.*, 2021, **23**(1), 144.
58 L. Morbidelli, S. Donnini and M. Ziche, *Curr. Pharm. Des.*, 2003, **9**, 521–530.
59 Y. Wang, W. Zhang, J. Yuan and J. Shen, *Mater. Sci. Eng., C*, 2016, **59**, 30–34.

60 Y. Wang, S. Chen, Y. Pan, J. Gao, D. Tang, D. Kong and S. Wang, *J. Mater. Chem. B*, 2015, **3**, 9212–9222.
61 N. Toda and T. Okamura, *Pharmacol. Rev.*, 2003, **55**, 271–324.
62 N. Maulik, *Antioxid. Redox Signaling*, 2006, **8**, 2161–2168.
63 C. Yang, N. Chung, C. Song, H. W. Youm, K. Lee and J. R. Lee, *Biofabrication*, 2022, **14**, 011001.
64 T. Murohara and T. Asahara, *Antioxid. Redox Signaling*, 2002, **4**, 825–831.